LBNL-63576

PREDICTING SPOT WELD BUTTON AREA WITH AN ULTRASONIC PHASED ARRAY

William B. Davis

Lawrence Berkeley National Laboratory
One Cyclotron Road, MS 46A-1123B, Berkeley CA 94720

ABSTRACT. In automobile manufacturing, the quality of spot welds joining thin mild steel sheets is assessed primarily by the diameter of the button remaining after destructive teardown, relative to the thickness of the sheets. To facilitate a comparison with destructive testing, several features of ultrasonic images of spot welds were assessed for their ability to predict weld button area. An experiment was performed in which representative weld test coupons were imaged with a prototype portable, hand-held phased array system, and then torn down destructively and their buttons measured. Features of the ultrasonic images were examined for their ability to predict the corresponding button areas. These features included: transmissive area; a frequency ratio proxy for reflectivity; and dimensions of the surface indentation caused by the welding electrode. Regression models with these explanatory variables predicting button area all achieve 95% or better fits. Button diameters were predicted with 95% confidence to an accuracy of 2-4 times the pitch of the array. These results indicate that the ultrasonic measurement system is sufficiently accurate for weld quality assessment.

Keywords: Spot Weld Inspection, Ultrasonic Phased Array, Signal and Image Processing, Quality Prediction
PACS: 43.35.Yb, 43.35.Zc, 81.70.Cv.

OBJECTIVE AND APPROACH

The objective of this effort is to develop software for automated spot-weld dimensioning and classification using a prototype portable, hand-held ultrasonic phased array. A sample of 75 test coupons was prepared by an industry partner which spanned the range of weld qualities, from stick or cold, to large or burnt. These coupons were imaged with the phased array and custom software, then torn down destructively and their buttons measured. Dimensions of the ultrasonic images were then utilized to predict the corresponding button areas with linear regression. The regression model also allows quantification of the sizing uncertainty.

PROBE SPECIFICATIONS AND EXPERIMENTAL DESIGN

The probed used is a linear array, with 80 channels and 16-channel aperture, resulting in 65 electronic signals. The probe is scanned mechanically perpendicular to the electronic scan, resulting in a 60x65 grid of signals. The pitch of the array is 0.25 mm, so the maximum area that can be imaged is 15x16.25 mm. The probe controller is an Omniscan OMNI-MX. The central ultrasonic frequency of the probe is 17 MHz, and the data acquisition rate is 50 MHz per channel. The probe system is portable and hand-held, and operates in pulse-echo mode.

The experimental sample consists of 75 test coupons in mild, galvanized steel. There are 25 coupons in each of three stackups: 0.8:0.8 mm, 0.8:1.8 mm, and 1.8:1.8 mm. For each stackup there are 5 coupons each with 5 target weld qualities: cold/stick, small, undersized, minimum acceptable, and large/burnt.

Three operators made ultrasonic measurements from the front and back surfaces. Additional measurements were made in a water tank, to examine the effects of the membrane used to retain the water column. Some repeat measurements were made by each operator. Over 500 measurements were made in total. One weld measurement consists of 60x65 or 3900 8-bit signals each with 320 time ticks.

SIGNAL AND IMAGE PROCESSING

Each signal is passed through several processing steps. Several summary statistics for the array of signals are displayed as images, and features of these images are used for weld button prediction. The main signal and image processing steps are illustrated in Figure 1.

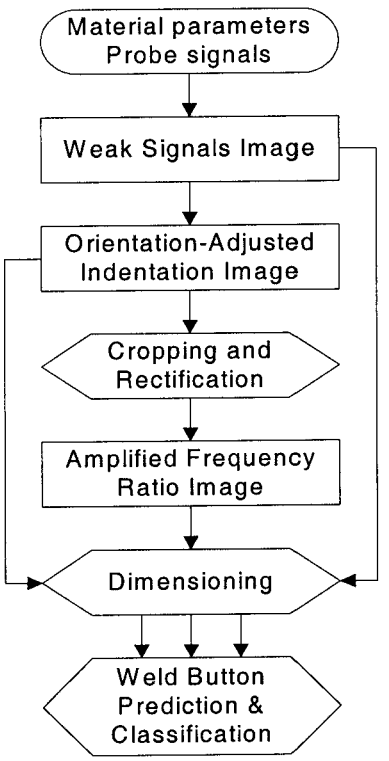

FIGURE 1. Signal and image processing and weld button area prediction software flowchart.

The rectangles in Figure 1 indicate the three images used for diagnosing and predicting weld quality. The weak signals image is used primarily as a preprocessing filter, the results of which determine if and how that signal is further processed. Dimensions of the indentation and amplified frequency ratio images are the primary diagnostics used by the weld button prediction software. These images are described in detail in the following subsections. How these images are used for the weld button predictions is described in the following section.

In addition to the 60x65 grid of probe signals the software further requires material and probe parameters as inputs. The material inputs required are ultrasound velocities in water and the material being probed, as well as nominal sheet thicknesses in the stackup. Probe parameters required include data acquisition sampling frequency and other signal parameters. The primary means by which a signal is diagnostic of weld quality is that good welds transmit ultrasonic energy, while bad welds often still reflect it at the welding interface. Examples of raw probe signals are provided in Figure 2.

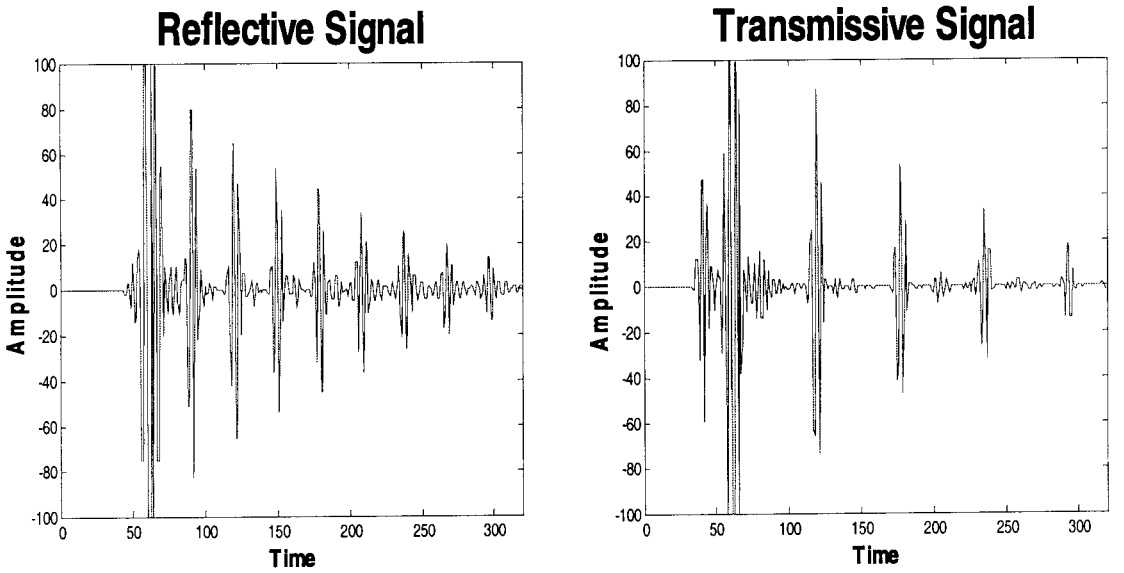

FIGURE 2. Raw signals generated by the probe. In an equal-thickness stackup, when the interface is reflective, the ultrasonic echoes are received at twice the frequency as when the interface is transmissive of ultrasound.

Weak Signals

The first operation performed on all signals is a pass through the weak signals filter. Weak signals can be due to poor coupling and scattering commonly seen around the edges of the welding electrode indentation. The weak signals filter bins the signals by the number of echoes discernible in that signal. A good signal has at least two discernible back-surface echoes. Figure 3 is a typical weak signals image. Black pixels have no discernible front-surface echo; dark grey pixels have no discernible back-surface echo; light grey pixels have one discernible back-surface echo; and, white pixels have more than one discernible back-surface echoes. Further signal processing for that pixel depends on category.

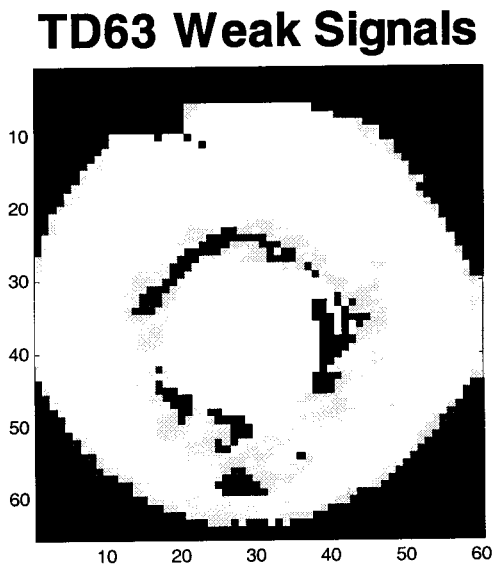

FIGURE 3. A typical weak signals image, with weak signals around the edge of the indentation.

Orientation-Adjusted Indentation

For signals with a discernible first front-surface echo (FFSE), the time-of-flight (ToF) to the FFSE measures the depth of the indentation, relative to the surrounding sheet. Because the probe unit is hand-held, in order to maximize signal strength in the weld the operator adjusts the orientation of the probe to be perpendicular to the bottom of the indentation. If the electrode tip is slanted instead of flat, then the bottom of the indentation is slanted, and this causes the orientation of the probe to become tilted relative to the surrounding sheets. Therefore in order to find the depth of the indentation relative to the surrounding sheets this tilt must be measured and subtracted from the raw ToFs to find the orientation-adjusted indentation. This is illustrated in Figure 4.

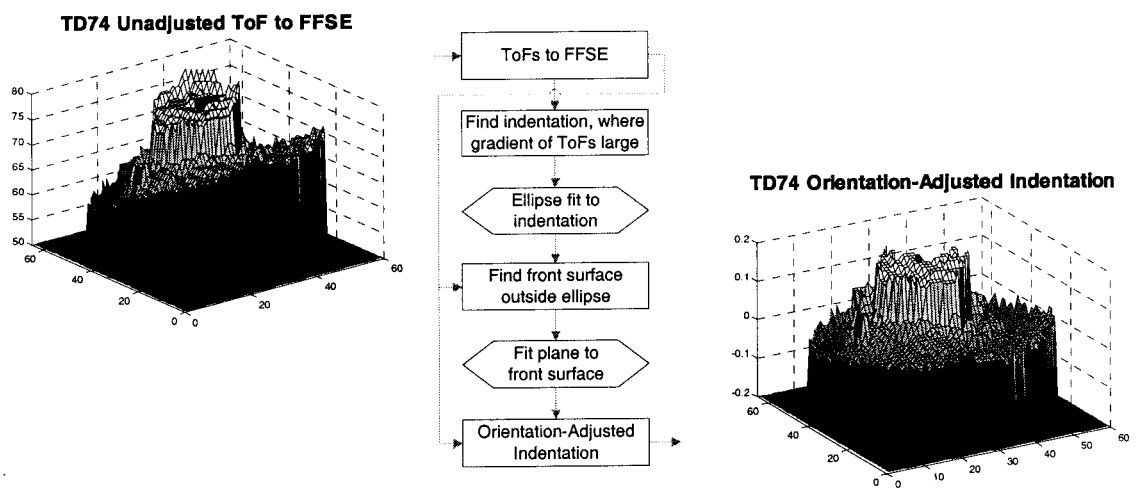

FIGURE 4. Measured indentation must be adjusted for orientation of the probe.

The raw ToFs to FFSE are simply the length of the head of the signal before it first exceeds some amplitude threshold. Typically the gain is adjusted so as to almost saturate the FFSE, without saturating the first interface echo (FIE), to maximize the number of discernible echoes received by the probe. Indexing the ToFs array by x and y, one way to approximate the gradient of the ToFs is to use the Laplacian, $\nabla\text{ToFs} = \sqrt{\Delta^2 x + \Delta^2 y}$. Where this gradient is large indicates the edges of the indentation.

To these edge points fit an ellipse using the method of Pilu et al. [1]. Representing a general conic section $F(\boldsymbol{a}, \boldsymbol{x}) = \boldsymbol{a} \cdot \boldsymbol{x} = ax^2 + bxy + cy^2 + dx + ey + f = 0$, where $\boldsymbol{a} = [a\ b\ c\ d\ e\ f]^T$ and $\boldsymbol{x} = [x^2\ xy\ y^2\ x\ y\ 1]^T$, then the constraint $4ac - b^2 > 0$ that restricts the conic to an ellipse can be rescaled and implemented as $\boldsymbol{a}^T\boldsymbol{C}\boldsymbol{a} = 1$, where the constraint matrix is

$$\boldsymbol{C} = \begin{bmatrix} 0 & 0 & 2 & 0 & 0 & 0 \\ 0 & -1 & 0 & 0 & 0 & 0 \\ 2 & 0 & 0 & 0 & 0 & 0 \\ 0 & 0 & 0 & 0 & 0 & 0 \\ 0 & 0 & 0 & 0 & 0 & 0 \\ 0 & 0 & 0 & 0 & 0 & 0 \end{bmatrix}$$

These authors prove that the ellipse that minimizes the sum of squared distances to data $\boldsymbol{D} = [\boldsymbol{x}_1\ \boldsymbol{x}_2 \ldots \boldsymbol{x}_n]$ solves the system

$$\begin{aligned} \boldsymbol{Sa} &= \lambda \boldsymbol{Ca} \\ \boldsymbol{a}^T\boldsymbol{Ca} &= 1 \end{aligned} \tag{1}$$

where $\boldsymbol{S}$ is the scatter matrix $\boldsymbol{D}^T\boldsymbol{D}$. The solution is found by considering the generalized eigenvectors. If $(\lambda_i, \boldsymbol{u}_i)$ solves (1) then so does $(\lambda_i, \mu\boldsymbol{u}_i)$ for any μ, and substituting into the constraint we can find the value of μ_i as $\mu_i^2\boldsymbol{u}_i^T\boldsymbol{Cu}_i = 1$, giving

$$\mu_i = \sqrt{\frac{1}{\boldsymbol{u}_i^T\boldsymbol{Cu}_i}} = \sqrt{\frac{1}{\boldsymbol{u}_i^T\boldsymbol{Su}_i}} \tag{2}$$

Finally setting $\boldsymbol{a} = \mu_i\boldsymbol{u}_i$ solves (1). These authors further prove that it is the unique positive eigenvalue that corresponds to the eigenvector solution to the problem of least-squares minimization ellipse fitting. This algorithm is also used for dimensioning the images produced by the probe software.

Once the indentation ellipse is fit, to the points outside this ellipse a plane is fit using bivariate ordinary least squares, and this plane is subtracted from the unadjusted ToFs and scaled by the sound velocity to yield the orientation-adjusted indentation. In addition to being directly useful for predicting spot-weld quality, the adjusted indentation is subtracted from the nominal sheet thickness, which improves the accuracy of further calculations requiring sheet thickness as input.

Integrated Amplified Frequency Ratio

The primary feature used to predict weld button area is derived from the frequency spectrum of the (cropped, rectified, amplified) signal. The head of the signal is cropped to just past the FFSE and prior the FIE, and the tail of the signal is also cropped so long as it does not exceed some small amplitude. The signal is then rectified by applying the absolute value operator and amplified over time at the rate of material attenuation. The frequency ratio is then calculated from this cropped, rectified, and amplified signal.

The frequency ratio can be sensitive to cropping. In particular, if the FFSE is not completely cropped then the calculated frequency ratio may change significantly and suddenly. Amplification was intended to make signals from different stackups more comparable, and is observed to improve the contrast in the output image.

The effect of rectification on the spectrum is to distinguish the low-frequency echoes from the high-frequency components due to the transducer function of the probe, which are generally in the vicinity of the central probe frequency. When rectified, the frequencies of the interface and back-surface echoes are identified as the first two peaks, at the lowest frequencies. The lowest frequency in the rectified signal is the arrival frequency of the back surface echoes, and the second-lowest frequency the arrival frequency of the interface echoes. This is illustrated in Figure 5.

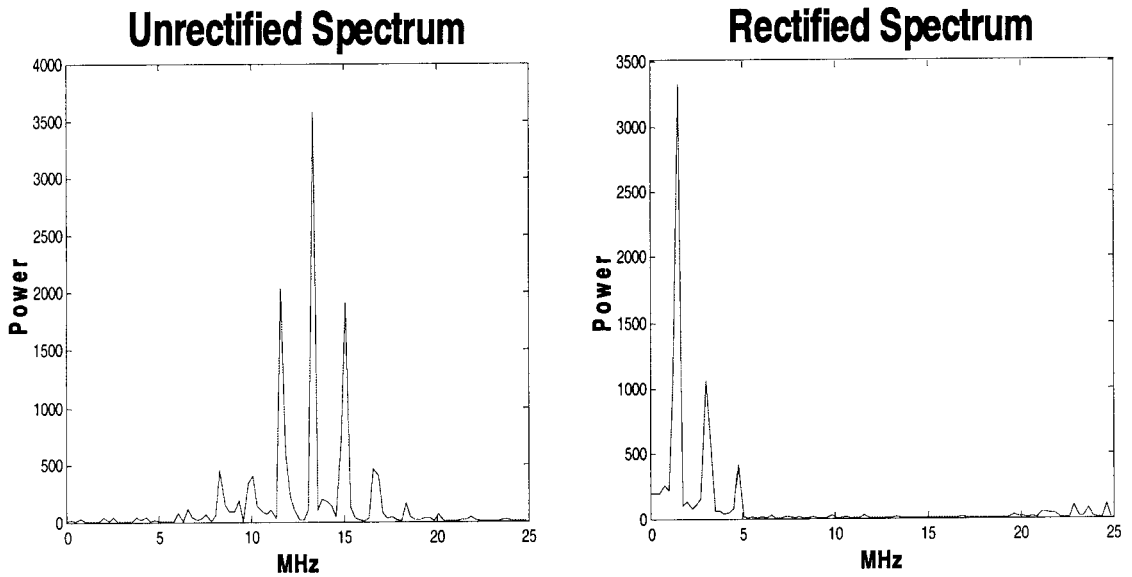

FIGURE 5. The effect of signal rectification on the spectrum.

The speed of 17 MHz ultrasound in mild steel is approximately 5.9 km/s (mm/μs), so the lower frequency peaks at about 1.5 and 3 MHz correspond with back-surface and interface travel paths of about 1.8 and 3.6 mm. This is illustrated in the spectrum in distance Figure 6. The distance spectrum is obtained from the frequency spectrum by inverting the abscissa and rescaling by the speed of sound in the medium.

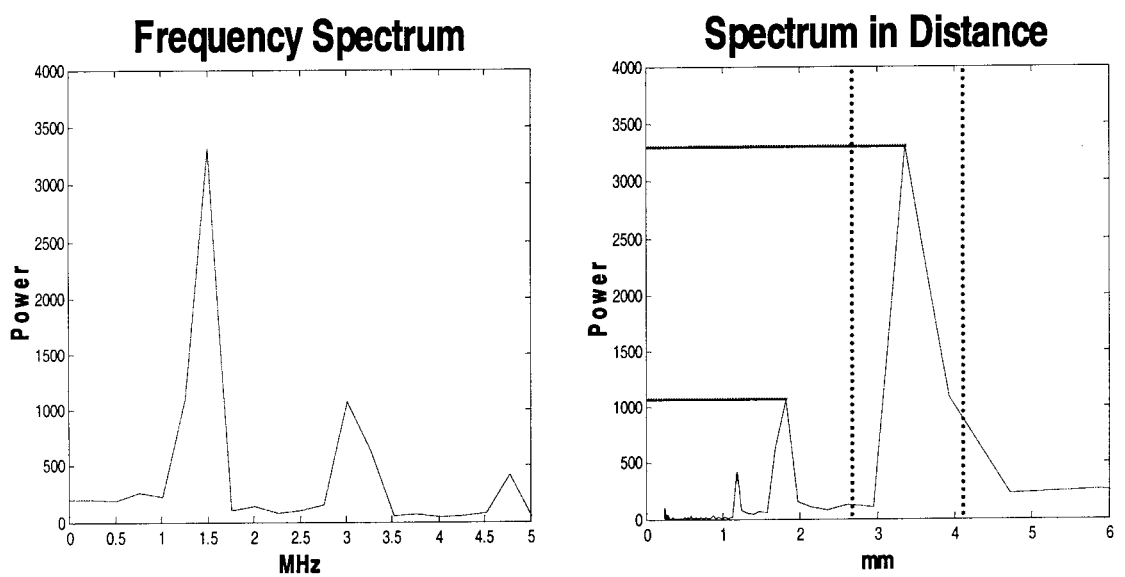

FIGURE 6. Distance representation of the spectrum. The frequency ratio illustrated indicates good transmission.

Calculating the frequency ratio entails finding the maximum spectral powers in windows around the expected back-surface and interface echoes, then forming a unitless ratio of these two peak powers. This is illustrated on the spectrum in distance in Figure 6, which has a frequency ratio of about 3. For each signal in the array, this frequency ratio is calculated, and assigned a color or grey value, resulting in an image. An example is provided in Figure 7.

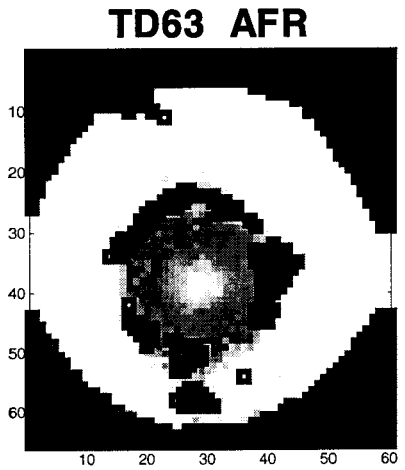

FIGURE 7. Amplified frequency ratio image with weak signals mask (black pixels) for a large/burnt donut weld.

The amplified frequency ratio (AFR) increases as the strength of the interface echo decreases, which is indicative of a transmissive weld bond. The AFR measure is independent of initial impulse, coupling, and gradual element failure, so long as these are all assumed to have a constant, multiplicative effect over time on the amplitude of the signal. That is, scaling the signal amplitude has no effect on the AFR.

Image Dimensioning

Image processing (including more ellipse fitting) automatically extracts features used as input into the prediction of weld button diameter: dimensions of the orientation-adjusted indentation and integrated amplified frequency ratio images.

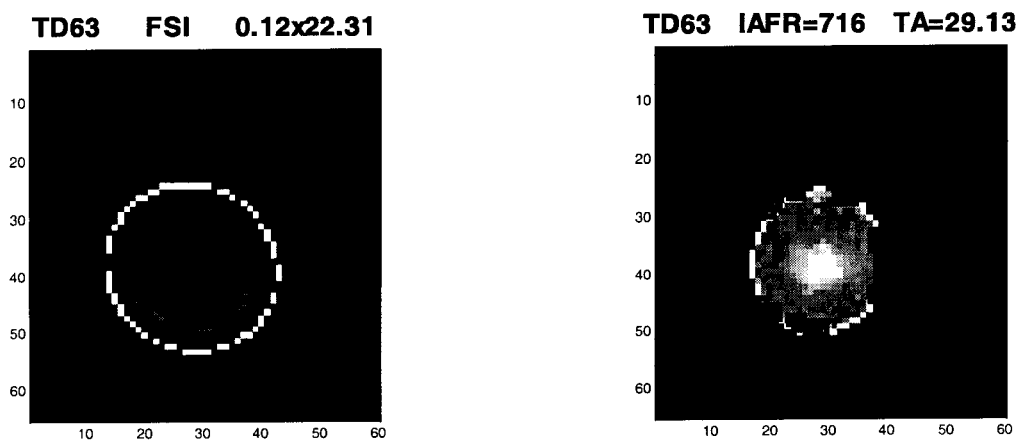

FIGURE 8. Orientation-adjusted indentation and integrated amplified frequency ratio dimensions.

The front-surface indentation (FSI) dimensions reported in mm average depth by sq. mm area. The transmissive area (TA) is the area over which the AFR exceeds some threshold, indicating transmission of ultrasound through the weld interface. IAFR is a sum of AFR in this area. Weak signals are assigned the average within the ellipse, and the same is done for white pixels beneath the transmission threshold for donut welds, because this improves prediction performance (donut welds still pull a large button).

PREDICTION OF BUTTON AREA FROM ULTRASONIC DATA

These image dimensions are then used as (quadratic, stepwise) regressors to predict button area measured after destructive teardown for each stackup. The resulting regressions, illustrated in Figure 9, have high goodness of fit, and always correctly predict weld quality.

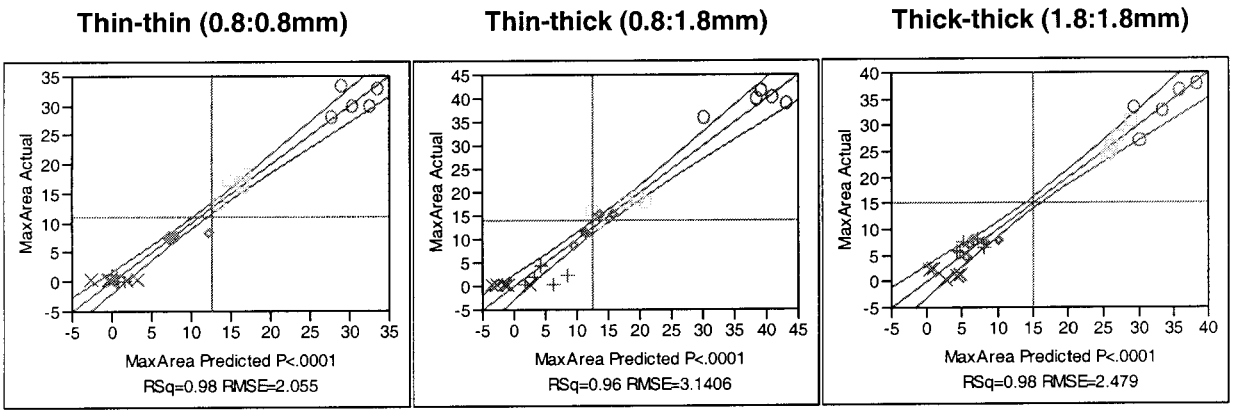

FIGURE 9. Regression models - button area predictions, by stackup.

The horizontal dotted line is the mean button area for that stackup, and the vertical line the accept/reject threshold. Perfect predictions lie exactly on the diagonal, and correct accept/reject classifications in the upper right and lower left quadrants. That each of the other two quadrants are blank indicate perfect prediction for these data. For all stackups, all cold/stick (X's) and large/burnt welds (O's) are correctly identified with confidence. For the best-performing model, the upper 95% confidence bound on the prediction at the accept/reject threshold is 0.4 mm, approaching the element pitch of the probe.

SUMMARY AND CONCLUSIONS

The button area regression prediction performance is very strong, with high goodness of fit, perfect weld quality classification, and demonstrated sizing accuracy of as little as less than twice the pitch of the array. These results, along with a preliminary gage repeatability and reproducibilty study, indicate that this system is sufficiently accurate for weld quality assessment.

ACKNOWLEDGEMENTS

This work was supported by the Department of Energy under Contract No. DE-ACO3-76SF00098, and performed at the Lawrence Berkeley National Laboratory. The author thanks Dr. Deborah L. Hopkins, and acknowledges the contributions of USCAR's NDE of Welded Metals Industry Steering Committee.

REFERENCES

1. A. Fitzgibbon, M. Pilu and R. B. Fisher, "Direct Least-Squares Fitting of Ellipses," *Pattern Analysis and Machine Intelligence*, Vol. **21** No. **5** (1999), pp. 476-80.